Accepted Manuscript

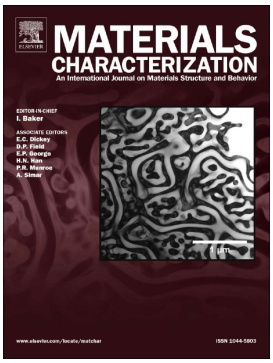

Study of structure of naturally aged aluminium after twist channel angular pressing

Lenka Kunčická, Radim Kocich, Vasyl Ryukhtin, Jonathan C.T. Cullen, Nicholas P. Lavery

PII: S1044-5803(18)33591-5
DOI: https://doi.org/10.1016/j.matchar.2019.03.045
Reference: MTL 9665

To appear in: *Materials Characterization*

Received date: 25 December 2018
Revised date: 23 February 2019
Accepted date: 29 March 2019

Please cite this article as: L. Kunčická, R. Kocich, V. Ryukhtin, et al., Study of structure of naturally aged aluminium after twist channel angular pressing, Materials Characterization, https://doi.org/10.1016/j.matchar.2019.03.045

Study of structure of naturally aged aluminium after Twist Channel Angular Pressing

Lenka Kunčická[a], Radim Kocich[b], Vasyl Ryukhtin[c], Jonathan C.T. Cullen[d], Nicholas P. Lavery[d]

a Institute of Physics of Materials, ASCR, Žižkova 22, 616 00 Brno, CZ

b VŠB-Technical University of Ostrava, 17. Listopadu 15, 708 33 Ostrava 8, CZ

c Nuclear Physics Institute, ASCR, Husinec - Řež 130, 250 68 Řež, CZ

d Materials Research Centre, College of Engineering, Swansea University Bay Campus, Fabian Way, Swansea, Neath Port Talbot, SA1 8QQ, UK

**Corresponding author: email:kuncicka@ipm.cz phone:+420532290371*

Abstract

Twist channel angular pressing (TCAP), the severe plastic deformation (SPD) technology developed recently to increase the efficiency of the imposed strain and its homogeneity within a single pass, is an effective process combining channel bending and twist extrusion in a single die. The presented study analyses the phenomena of substructure development, precipitation, structural units' orientations, and the occurrence of residual stress, as well as electric resistivity and microhardness, in commercial purity aluminium naturally aged for two years at room temperature after processing via single pass TCAP. The results are compared with the findings for the TCAP sample right after processing; selected results are also compared with the results for the sample after TCAP and one year of natural ageing, and with a sample processed by conventional ECAP. The analyses showed the substructure to recover substantially, the grain size decreased to submicron size. The residual stress within the grains introduced by the energy accumulated via the severe imposed strain relaxed significantly by the structure restoration, as well as by intensive precipitation. The aged TCAP sample specific electric resistivity was comparable to the resistivity of the original commercially pure aluminium (2.652E-05 and 2.635E-05 $\Omega \cdot mm^2 \cdot m^{-1}$, respectively), however, the microhardness mapping showed increased mechanical properties with homogeneous distribution.

Keywords: twist channel angular pressing; aluminium; electron microscopy; neutron diffraction; electric resistivity; precipitation

1. Introduction

Severe plastic deformation (SPD) methods are designed to effectively refine structural units of the processed materials via imposing significant plastic shear strain, which results in the enhancement of the mechanical as well as physical properties [1–4]. The methods are generally characterized as continuous, and discontinuous [5] and can be used to process various types of samples from bulk materials and continuous billets [6], through plates, sheets, rods and tubes [7], to surfaces and thin cross-sections [8]. Nevertheless, the paths along which the strain is imposed – depending on the particular die geometry (and possible deformation route if multiple passes are applied) and influencing significantly the overall impact of processing on the final material properties – vary for the individual methods [9–11].

Although some of the SPD methods do not feature many degrees of freedom for the strain path to be varied, such as high pressure torsion [12], or accumulative roll bonding [13], some methods are flexible. One of the most popular SPD technologies, the strain path for which is variable, is equal channel angular pressing (ECAP) [14–16]. For this technology, various multi-pass routes, the most known of which are A, Ba, Bc and C, can be applied [17] (route Bc has been considered to be the most favourable from the viewpoints of grain refinement efficiency and achievement of equiaxed grains [18]).

In order to make the process more effective, several ECAP modifications have been introduced to satisfy the demand of higher and more homogeneous strain accumulation during a single pass (which generally provides increased grain refinement and improves properties during a single pass) [19–22]. Among such modifications are for example ECAP with implemented partial back pressure (ECAP-PBP) featuring local necking in the outlet channel [22], non-equal channel angular pressing (NECAP [23]), ECAP with multiple deformation zones – twists and bends (TCMAP [19]), and, last but not least, the recently developed twist channel angular pressing (TCAP) technology featuring one twist section and one bending

section [24]. Numerical analyses by Kocich et al. [25] predicted a single TCAP pass to feature the effective strain of ~ 3, which is more than twice as high as for a single ECAP pass, and also higher than for two pass ECAP via all the basic routes. Previously performed studies also showed that the homogeneity of the imposed strain is more advantageous than for single and double pass ECAP [16,18]. The experimental evaluation of TCAP deformation routes efficiency is complex and depends on the particular investigated structure parameter or property [10]. Contrary to ECAP, single pass TCAP imposes the shear strain into the material along three independent shear planes, which results in significant grain refinement due to increased dislocation density within the cell walls and decreased cell size [26]. Nevertheless, the effect of time on TCAP-processed materials was not investigated so far.

This study focuses on the structure changes within commercial purity (CP) aluminium processed via single pass TCAP after one year and two years of natural ageing at room temperature. Dislocations, as well as grain boundaries and precipitates were observed via SEM and TEM, while overall structure changes, primarily as concerns structural units' orientations and grains relaxation (i.e. the possible presence of residual stress), were also analysed via neutron diffraction. The whole study is supplemented with specific electric resistivity measurements and thorough microhardness mapping documenting the favourable effect of TCAP on the imposed strain homogeneity.

2. Experimental material and procedures

CP aluminium of 99.17 purity (the exact composition determined via electron dispersive spectroscopy was Al + 0.625 Fe; 0.120 Si; 0.020 Zn; 0.020 Cu; 0.015 Mn; 0.015 Mg; 0.015 Ti) square billets with the dimensions of 12x12x120 mm^3 were heat treated at 400 °C for 1 hour and extruded with the speed of 3 mm/s at room temperature on a hydraulic press via single pass TCAP. The MoS_2 substance was used as a lubricant. For comparison, another billet was pressed via single pass ECAP under identical processing conditions.

After extrusion, samples for subsequent analyses were cut using electrical discharge machining and water jet cutter [27]. The samples for SEM observations were mechanically ground and pre-polished using SiC grinding papers and finally polished electrolytically. The foils for TEM were prepared using a twin jet electro polishing equipment. SEM analyses on cross-sectional cuts perpendicular to extrusion axes of the processed billets were carried out using a Tescan Lyra 3 FIB/SEM microscope with a NordlysNano EBSD detector; the scan steps for EBSD analyses were 0.1-0.5 μm. TEM images were acquired with a Jeol 2100F device. SEM scans were also used to provide a brief insight into the residual stress development via the ATOM LEM 3 software [28].

Neutron diffraction analyses were performed by the small angle neutron scattering (SANS) technology. SANS measurements were conducted at V4 instrument of Helmholtz Zentrum Berlin (*www.helmholtz-berlin.de*). The TCAP-processed sample (aged for two years), several locations at which were analysed (as depicted in Fig. 1a), was mounted at 2 metres distance from the detector (SD = 2 m) and exposed to monochromatic (λ = 5 Å) and collimated neutron beam. Aperture of 4.5 mm round cross section was used for all the studied locations of the 6 mm thick axially cut half sample. The data were background corrected via empty beam and cadmium standard and calibrated using 1 mm water standard by the BerSANS program. The peaks of azimuthally averaged intensities correspond to the orientation of the longer sample axis inclined by 10 ° in the CCW direction from the horizontal line.

The electric resistivity investigations were performed at room temperature with 100 mm long samples of the unprocessed material, billet right after TCAP, one-year-aged billet, and two-years-aged billet. The measurements were performed using a Metex MS-9170 equipment, the electric voltage U by which was determined. Subsequently, the specific electric resistivity ρ was computed using the $\rho = U \cdot S/I \cdot L$ formula, where S was billet cross-sectional area, I was current, and L was measured billet length.

The microhardness was determined using a Bruker Wilson Vickers VH3300 Hardness Tester at the MACH 1 centre and COMET at Swansea University, with a force of 1 kgf·mm^{-2} applied to the sample. Before the measurements, the sample was polished using 1μm diamond paste to remove the surface residuals produced by cutting tools. A total of 285 indents were preformed to produce a map surface of the sample (Fig. 1b). The distance between each indent was 1 mm and the offset distance from the bend edge to first row and column of indents was 1 mm.

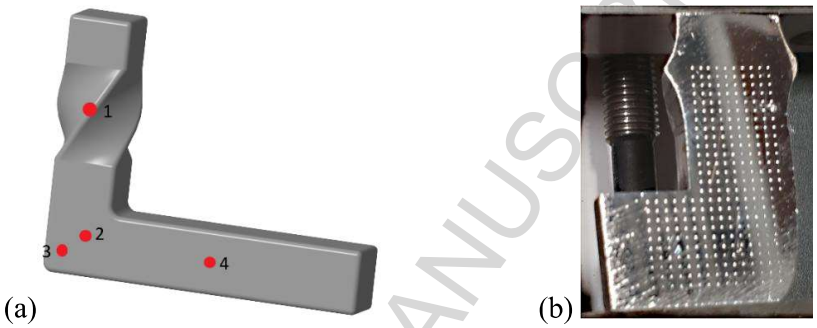

Fig. 1: Schematics of TCAP billet with locations for neutron diffraction analyses, individual scanning planes were perpendicular to extrusion axis in each individual point, for points 2 and 3 scanned plane crossed both points (a); photo of TCAP billet with microhardness indents (b).

In summary, three billets of CP aluminium were processed via a single pass TCAP and one billet was processed via a single pass ECAP. Out of the TCAP-ed ones, the first billet was examined right after processing, the second one after one year of natural ageing, and the third one was aged at room temperature for two years. After ageing (or after processing for the first TCAP-ed one and for the ECAP-ed one), the billet was subjected to the measurements of electric conductivity and then axially cut to two halves and subjected to small angle neutron scattering and microhardness measurements. Finally samples were subjected to scanning and transmission electron microscopy observations of structures. However, in order to keep the manuscript within a reasonable length, only selected results for the two-years-aged sample are compared with the results acquired for the other billets.

3. Results and discussion

3.1 Grain Size

The unprocessed aluminium exhibited relatively coarse grains with the average diameter of slightly less than 40 μm. However, several grains had the diameter larger than 100 μm. This result is documented via the EBSD scan depicted in Fig. 2a showing grains of the unprocessed Al featuring mostly high angle grain boundaries (HSGB), which are highlighted in green, and the corresponding grain size distribution chart in Fig. 2b. After a single pass ECAP, the grains refined down to the average size of ~ 7 μm (Fig. 2c). Significant grain refinement was recorded after a single pass TCAP; the average grain diameter for TCAP sample was smaller than 6 μm, and, by the effect of the severe imposed strain, almost 75 % of the grains had the diameter smaller than 5 μm (see the grain size distribution in Fig. 2d). The results prove that the grain refinement efficiency induced by a single pass TCAP was not only higher than for a single pass ECAP, but also higher than for two passes of ECAP performed by routes A and even Bc (see refs. [18,26] for comparison of grain sizes and more detailed descriptions of grains orientations and textures). This supposition was further confirmed by the analyses of the TCAP sample subjected to natural room temperature ageing; Fig. 2e depicts the grain size distribution for the two-years-aged TCAP sample, the average grain diameter for this material state was smaller than 1 μm. The imposed energy thus evidently imparted significant substructure development and resulted in the formation of ultra-fine-grained (UFG) structure featuring also new recrystallized grains, which is documented by Fig. 2f showing recrystallized grains that formed during post-process recrystallization (green colour), newly occurring subgrains (yellow colour), and originally deformed structure depicted in red colour. The high imposed strain also supported post-process development of precipitates (white unindexed points in Fig. 2f and Section 3.2).

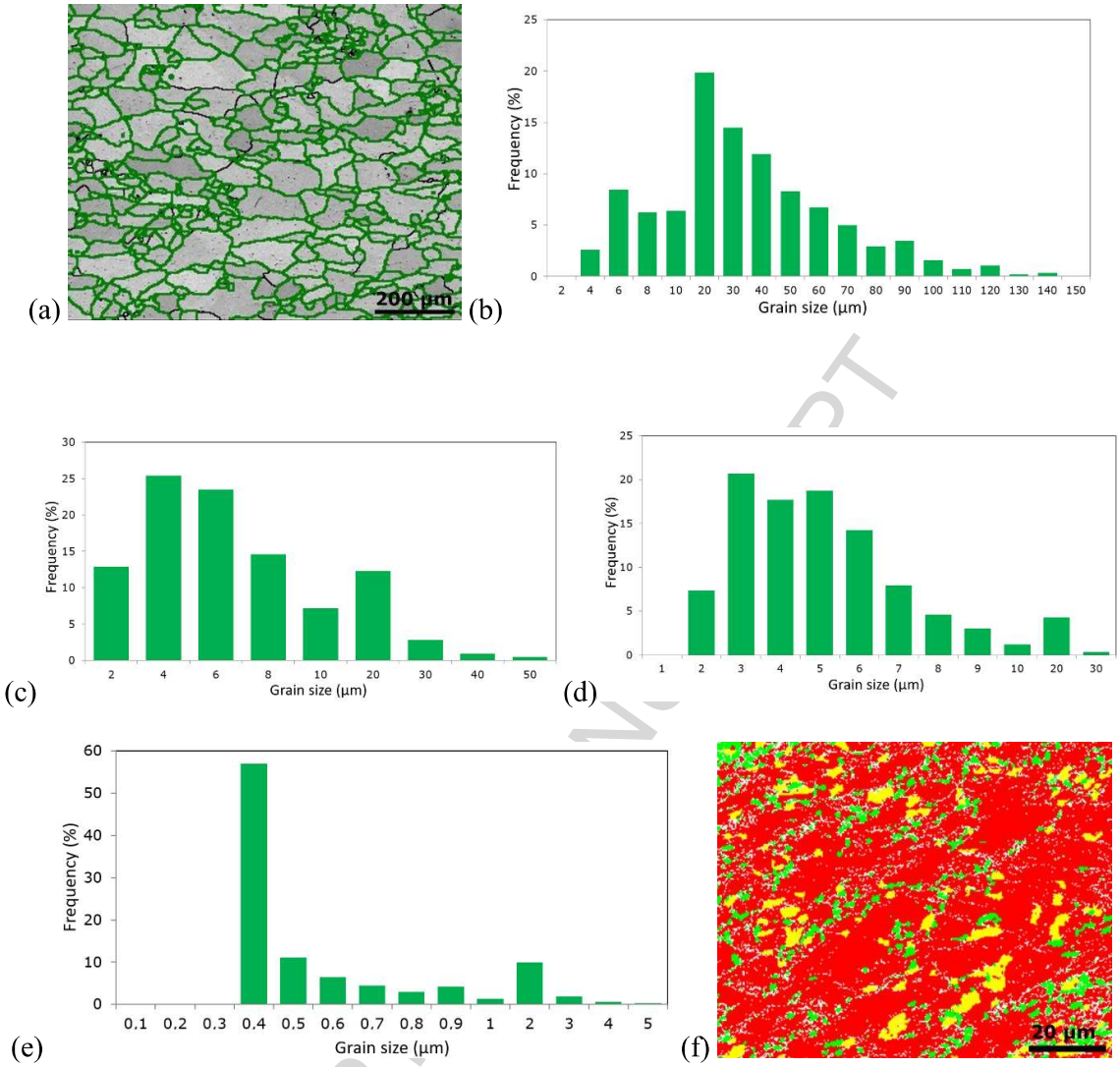

Fig. 2: EBSD scan of unprocessed material, HAGBs highlighted in green (a); grain size distribution for unprocessed state (b); grain size distribution after single pass ECAP (c); grain size distribution after single pass TCAP (d); grain size distribution after TCAP, two-years-aged (e), recrystallized fraction for two-years-aged TCAP sample (f).

The efficiency of the process is primarily given by the character of the technology. The process involves two stages of imposing shear strain [26]. In the first stage, the peripheral regions of the processed billet are deformed by the twist section, while the second stage consists of imposing the strain to the central region of the billet via the bending section.

Single pass TCAP thus introduces novel and very efficient combination of three independent strain paths inducing a high volume of lattice distortions acting as obstacles for dislocations movement and nucleation sites for new grains [29].

3.2 Substructure and residual stress

The results of SEM observations were further supported by TEM analyses confirming the substantial substructure development and formation of new recrystallized grains in the aged samples. Fig. 3a depicts substructure of TCAP sample right after processing. The image shows dislocation cells and walls and newly forming subgrains. Structures of one-year-aged samples processed by ECAP and TCAP are depicted in Figs. 3b and 3c, respectively. As can be seen, the ECAP sample featured mostly recovered dislocations-free grains, while the TCAP sample exhibited substantial substructure development – dislocation walls and dislocation tangles (A), newly occurring recrystallized grains (B), and precipitates (C) – introduced by the severe imposed strain.

The Bragg equation ($2d \cdot \sin\theta = 2\lambda$) [30] implies that the structural units (grains, subgrains) featuring identical crystallographic orientations have identical diffraction intensities in TEM scans. Based on this presupposition, the identical shades of grey of majority of the grains within the one-year-aged ECAP sample point to their identical orientations and therefore to the presence of deformation texture after one year of natural ageing [31]. On the other hand, the TEM scan of one-year-aged TCAP sample featured a palette of shades of grey, which points to the development of subgrains and also new grains with randomized orientations, which decreases the deformation texture intensity.

After another year of natural ageing, the substructure of the two-years-aged sample exhibited reorganisation into a large number of new grains featuring HAGBs (Fig. 3d and Fig. 2f in Section 3.1), as well as the occurrence of a large number of fine precipitates, which can

also be seen in the SEM scan in Fig. 4a (white points) and more in detail in the TEM scan in Fig. 4b. According to the TEM analyses, the precipitated particles were composed of aluminium with Fe, and minor portions of Si, Mn and Cu. The chemical compositions of several distinguishable precipitates depicted with numbers in Fig. 4b are depicted in Table 1.

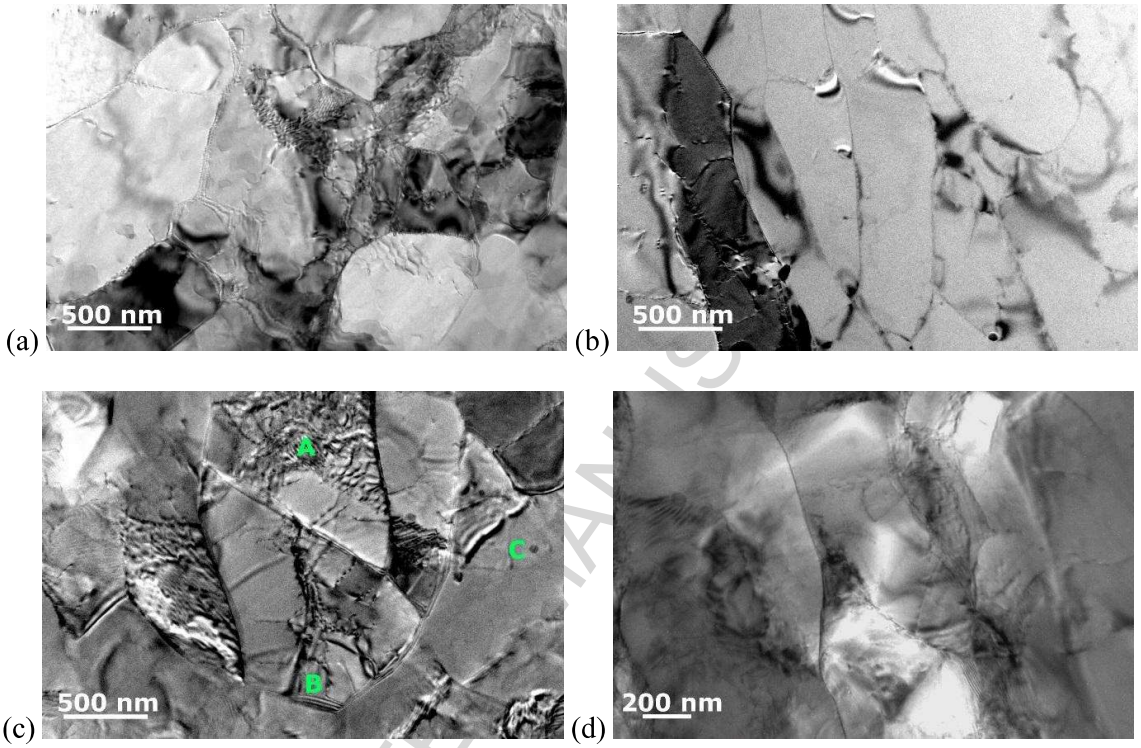

Fig. 3: TEM images taken from samples: TCAP after processing (a); one-year-aged ECAP (b); one-year-aged TCAP (c); two-years-aged TCAP (d).

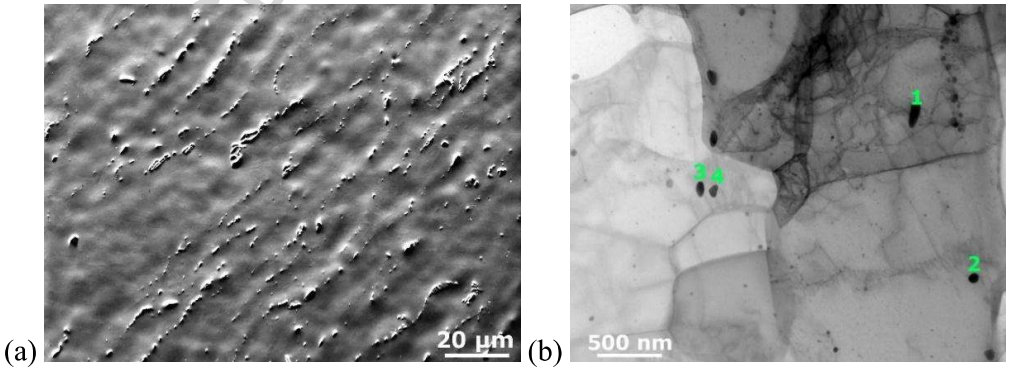

Fig. 4: Development of precipitates within two-years-aged TCAP, SEM image (a); TEM image (b).

Table 1: Chemical compositions of precipitates depicted in Fig. 4b.

Precipitate	chemical composition in wt. %				
no.	Al	Fe	Si	Mn	Cu
1	83.6	11.6	2.6	1.9	0.3
2	88.2	8.4	2.1	1.4	0
3	88.2	7.3	2.5	1.0	1.0
4	89.8	7.2	1.4	1.3	0.3

Substructure reorganization can also manifest as changes in the intrinsic properties, one of the most characteristic of which is the residual stress [32]. Residual stress within the structure can develop as a result of a high imposed strain and, except specialized applications, is unfavourable since it can promote cracks propagation and eventually lead to deteriorated longevity of the final products. As can be seen in Fig. 5a, the TCAP structure right after processing featured high misorientations within majority of the grains, which was the result of the very high imposed strain causing high accumulated energy and introducing non-equilibrium material state (according to the scale in the Figure, red colour signifies the misorientation of neighbouring scanned points up to 15 degrees).

After two years of ageing, the portion of high misorientations decreased significantly; the material thus naturally attempted to achieve the equilibrium state in which it was before SPD processing. Evidently, especially the locations featuring high accumulated energy and high misorientations after processing were preferential to restore after ageing (Fig. 5b). The central region of the scan, however, still exhibited high grains misorientations, indicating imperfect restoration. This finding corresponds to the results of the analysis of recrystallized portion depicted in Fig. 2f (section 3.1), in which the largest portion of newly recrystallized grains featuring HAGBs was also found in the peripheral regions of the scan, while the central region still featured mainly deformed structure and newly forming subgrains.

(a) 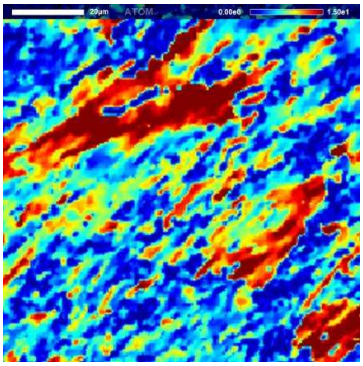 (b) 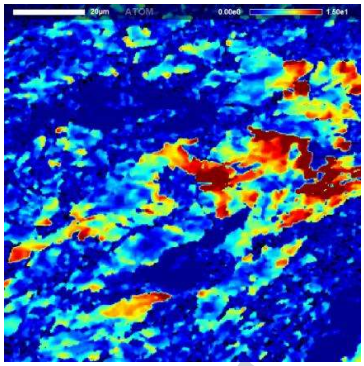

Fig. 5: Residual stress within TCAP sample; after processing (a); after two years of natural ageing (b).

3.3 Neutron diffraction analyses

The two-dimensional SANS patterns measured at SD=2 m showed scattering anisotropies in the examined locations within the two-years-aged TCAP sample. The anisotropies in the measured locations were correlated via azimuthal averaging. As can be seen in Fig. 6a, the intensities slightly increased in the regions with angles of ~ 90° and 270° for planes superimposed through points 1 and 4. This finding signifies that the scattering objects were elongated in the directions parallel to the extrusion axis (positioned vertically during the measurements in the examined locations).

The elongation of the scattering objects in the extrusion direction for the plane superimposed through point 1 can be attributed to the twist character of this part of the die, the strain within which is imposed to the extruded billed inhomogeneously from the billet axis towards its peripheral regions. The scattering objects align to the preferential orientations according to the paths the strain along which is imposed into the material [26], which eventually causes the formation of texture. This is documented in Fig. 6b, the halo on the SANS pattern in which is deformed to an ellipse (in an ideal case of random orientations of the scattering objects, the halo has a circular character) [33]. However, no such behaviour was observed for the data collected from the plane superimposed through points 2 and 3. This can

be caused either by the fact that the contributions of anisotropic scatterings in superposition smear out the intensity peaks, or by the absence of preferred orientations of the particles. The preferential orientations (texture) of the scattering objects developing during passing of the billet through the twist part of the die diminished (to a certain extent) by the effect of the deformation zone within the bend, the strain in which is imposed with the highest intensity to the central (axial) region of the billet. This eventually homogenizes the overall effect of strain, since the strain was imposed the most intensively to the peripheral regions of the billet in the twist zone. Nevertheless, for the plane superimposed through point 4, the results were similar to the findings for point 1 (Fig. 6a). In this location (behind the bending part of the die), the material was primarily sheared by the effect of different velocities of material flow along the outlet channel. The material layers in the vicinity of the bottom part of the channel are delayed when compared to the material layers in the vicinity of the upper part of the outlet channel and their trajectory is longer (depending on the outer radius of the channel bend defined by angle Ψ) [5, 11]. This fact causes the upper region of the billet to flow faster than the bottom region, which results in the elongation of the scattering objects. However, this effect is not as intensive as the effect of the twist, as can be seen in Fig. 6c, the SANS halo for the plane superimposed through point 4 in which is shown. The scattering in areas with low region momentum transfer vector Q originated from large inhomogenities, most probable residual stress, the presence of which even after two years of natural ageing was still registered (Fig. 5b).

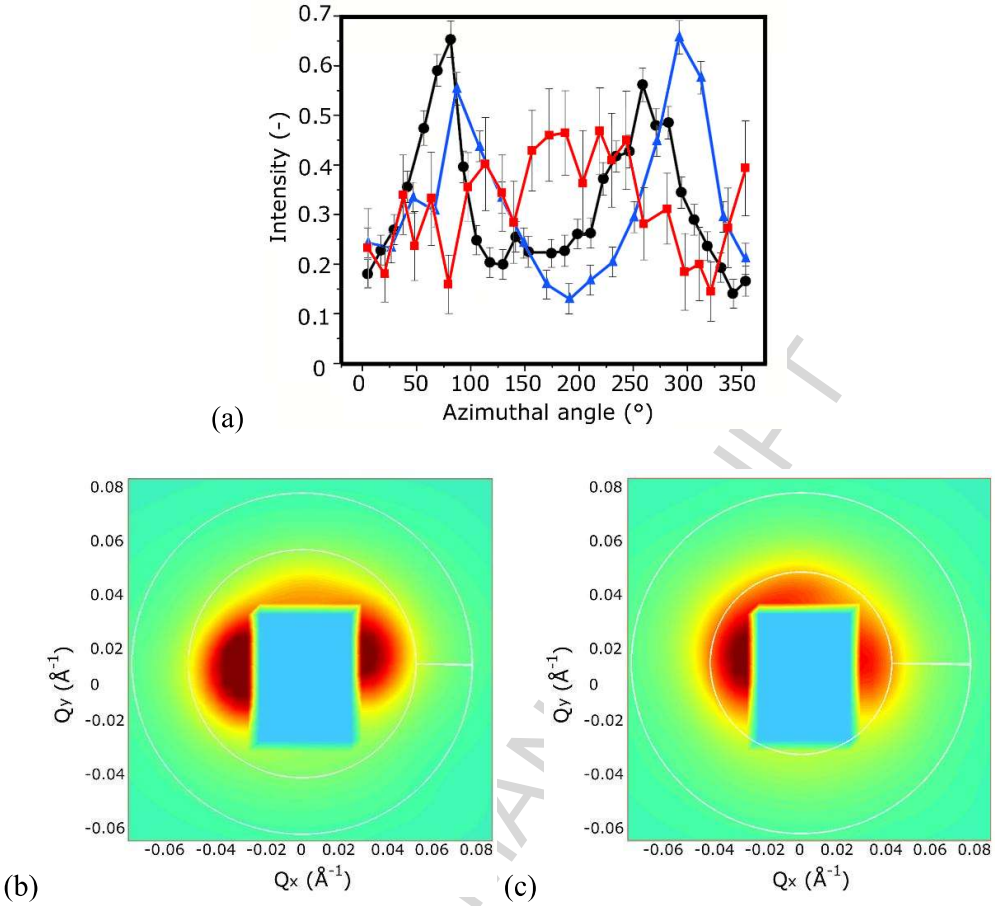

Fig. 6: Azimuthally averaged scattered data (a); SANS pattern from twist region (plane superimposed through point 1) (b); SANS pattern from plane superimposed through point 4 in outlet channel (c).

3.4 Electric resistivity

The results of measurements of specific electric resistivity for the TCAP sample right after processing, after one year of ageing, and after two years of ageing are depicted in Table 2. As can be seen, the resistivity increased after processing, and again after one year of ageing. On the other hand, after another year of ageing (two-years-aged sample), the resistivity decreased, i.e. the conductivity increased. These facts can be explained via the occurring structural phenomena. The resistivity increase after processing can be attributed to the significant increase in dislocation density and the precipitation induced by the severe imposed strain [24].

After one year of ageing, the accumulated energy caused the precipitates to develop in a greater extent, which lead to a further increase in resistivity [34]. The two-years-aged sample featured substantial precipitation, too. However, the structure also exhibited significant restoration resulting in the presence of new dislocations-free grains – this was also observed for the one-year-aged sample, but in a lesser extent [35]. In addition, the occurring structural changes also influenced the distribution of precipitates. These phenomena eventually manifested as a decrease in the specific electric resistivity and residual stress (Section 3.2).

Table 2: Electric resistivity of TCAP samples in various conditions

Sample state	Electric resistivity ($\Omega \cdot mm^2 \cdot m^{-1}$)		
	average value from three measurements	standard deviation	trend
original Al	2.635E-05	1.101E-07	-
after single pass TCAP	2.707E-05	6.371E-08	↑
one-year-aged TCAP	2.720E-05	1.638E-08	↑
two-years-aged TCAP	2.652E-05	1.395E-08	↓

3.5 Microhardness

The map of microhardness for the two-years-aged TCAP sample is depicted in Fig. 7. The figure shows the values measured on the axial cut surface plotted against distance; the colour bar shows the magnitude of the hardness in the scale from blue (lowest) to red (highest). As can be seen, the highest values were detected after the sample had passed the bending zone (i.e. in the outlet channel). The uniformity of the values across the cross section is evident, which confirms the homogenizing effect of the three independent strain paths, as documented previously via experimental characterizations, as well as numerical predictions [18,25,26,36]. The comparison of the measured values with the average values for the undeformed material (44.6 HV) and the sample right after processing (91.4 HV) [18] imparts that the effect of

restoration processes occurring during the two years prevailed over the effect of precipitation (especially in the region in which the sample only passed through the twist – before the bend – due to the lower accumulated energy). Nevertheless, the effect of precipitation still ensured the hardness to be higher than of the original material. The HV results also confirm the results of electric resistivity measurements (Section 3.4).

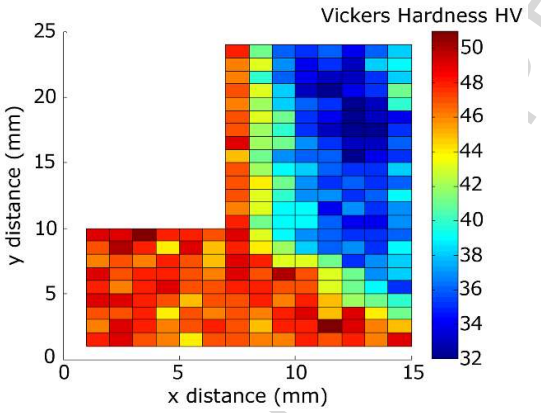

Fig. 7: Microhardness values across the two-years-aged sample.

4. Conclusions

The presented study characterized the structure development within commercial purity aluminium processed via twist channel angular pressing (TCAP) and subsequently aged naturally for two years. For comparison, selected results were compared to identical billets processed via TCAP and aged for one year, and via conventional ECAP. The results showed that the effective structure refinement after TCAP also implied other positive effects; besides the homogenous increase in the mechanical properties, the electric resistivity was influenced as well. Evidently, severe plastic deformation imparts the development of non-equilibrium structures. However, their stability is limited and the structures tend to return to the equilibrium states in time. As a result of the intensive accumulated energy within the Al after TCAP, the natural ageing led to a gradual reduction of residual stress, further structure

refinement and the development of new grains defined with high angle boundaries. Therefore, the material after two years of ageing featured ultra-fine-grained structure with increased mechanical properties and improved electric conductivity when compared to the state right after processing. In other words, the material featured an advantageous combination of mechanical and electric properties, which is favourable e.g. for electric conductors. For industrial purposes, optimization of accelerated ageing regimes which can speed up the whole fabrication process would be favourable; such study is being prepared for the following manuscript.

Acknowledgement

The authors acknowledge the 19-15479S Project of the Grant Agency of the Czech Republic.

Data availability statement

The raw data required to reproduce this study cannot be shared at this time as the data are part of an ongoing study.

References

[1] Y. Cao, S. Ni, X. Liao, M. Song, Y. Zhu, Structural evolutions of metallic materials processed by severe plastic deformation, Mater. Sci. Eng. R Reports. 133 (2018) 1–59. doi:10.1016/j.mser.2018.06.001.

[2] T. Mineta, H. Sato, Simultaneously improved mechanical properties and corrosion resistance of Mg-Li-Al alloy produced by severe plastic deformation, Mater. Sci. Eng. A. 735 (2018) 418–422. doi:10.1016/J.MSEA.2018.08.077.

[3] C.G. Figueroa, R. Schouwenaars, J. Cortés-Pérez, R. Petrov, L. Kestens, Ultrafine gradient microstructure induced by severe plastic deformation under sliding contact conditions in copper, Mater. Charact. 138 (2018) 263–273. doi:10.1016/J.MATCHAR.2018.02.017.

[4] L. Kunčická, T.C. Lowe, C.F. Davis, R. Kocich, M. Pohludka, Synthesis of an Al/Al2O3 composite by severe plastic deformation, Mater. Sci. Eng. A. 646 (2015) 234–241. doi:10.1016/j.msea.2015.08.075.

[5] V. Segal, Review: Modes and processes of severe plastic deformation (SPD), Materials (Basel). 11 (2018). doi:10.3390/ma11071175.

[6] P. Lukac, R. Kocich, M. Greger, O. Padalka, Z. Szaraz, Microstructure of AZ31 and AZ61 Mg alloys prepared by rolling and ECAP, Kov. Mater. Mater. 45 (2007) 115–120.

[7] M. Arzaghi, J.J. Fundenberger, L.S. Toth, R. Arruffat, L. Faure, B. Beausir, et al., Microstructure, texture and mechanical properties of aluminum processed by high-pressure tube twisting, Acta Mater. 60 (2012) 4393–4408. doi:10.1016/j.actamat.2012.04.035.

[8] Y. Hovanski, J.E. Carsley, K.D. Clarke, P.E. Krajewski, Friction-Stir Welding and Processing, JOM. 67 (2015) 996–997. doi:10.1007/s11837-015-1397-5.

[9] C.F. Gu, L.S. Tóth, M. Arzaghi, C.H.J. Davies, Effect of strain path on grain refinement in severely plastically deformed copper, Scr. Mater. 64 (2011) 284–287. doi:10.1016/J.SCRIPTAMAT.2010.10.002.

[10] R. Kocich, J. Fiala, I. Szurman, A. Macháčková, M. Mihola, Twist-channel angular pressing: effect of the strain path on grain refinement and mechanical properties of copper, J. Mater. Sci. 46 (2011) 7865–7876. doi:10.1007/s10853-011-5768-1.

[11] A. Gholinia, P.B. Prangnell, M. V. Markushev, Effect of strain path on the development of deformation structures in severely deformed aluminium alloys processed by ECAE, Acta Mater. 48 (2000) 1115–1130. doi:10.1016/S1359-6454(99)00388-2.

[12] L. Kunčická, R. Kocich, Comprehensive Characterisation of a Newly Developed Mg–Dy–Al–Zn–Zr Alloy Structure, Metals (Basel). 8 (2018) 73–88. doi:10.3390/met8010073.

[13] R. Kocich, A. Macháčková, F. Fojtík, Comparison of strain and stress conditions in conventional and ARB rolling processes, Int. J. Mech. Sci. 64 (2012) 54–61. doi:10.1016/j.ijmecsci.2012.08.003.

[14] R. Kocich, M. Kursa, A. Macháčková, FEA of Plastic Flow in AZ63 Alloy during ECAP Process, Acta Phys. Pol. A. 122 (2012) 581–587.

[15] M.S. Shadabroo, A.R. Eivani, H.R. Jafarian, S.F. Razavi, J. Zhou, Optimization of interpass annealing for a minimum recrystallized grain size and further grain refinement towards nanostructured AA6063 during equal channel angular pressing, Mater. Charact. 112 (2016) 160–168. doi:10.1016/j.matchar.2015.12.018.

[16] R. Kocich, M. Greger, A. Macháčková, Finite element investigation of influence of selected factors on

ECAP process, in: Met. 2010 19th Int. Metall. Mater. Conf., Tanger Ltd., 2010: pp. 166–171.

[17] V. V Stolyarov, Y.T. Zhu, I. V. Alexandrov, T.C. Lowe, R.Z. Valiev, Influence of ECAP routes on the microstructure and properties of pure Ti, Mater. Sci. Eng. A. 299 (2001) 59–67.

[18] R. Kocich, L. Kunčická, P. Král, A. Macháčková, Sub-structure and mechanical properties of twist channel angular pressed aluminium, Mater. Charact. 119 (2016) 75–83. doi:10.1016/j.matchar.2016.07.020.

[19] R. Kocich, L. Kunčická, A. Macháčková, Twist Channel Multi-Angular Pressing (TCMAP) as a method for increasing the efficiency of SPD, IOP Conf. Ser. Mater. Sci. Eng. 63 (2014) 12006. doi:10.1088/1757-899X/63/1/012006.

[20] C.F. Gu, L.S. Toth, Texture development and grain refinement in non-equal-channel angular-pressed Al, Scr. Mater. 67 (2012) 33–36. doi:10.1016/j.scriptamat.2012.03.014.

[21] M.H. Paydar, M. Reihanian, E. Bagherpour, M. Sharifzadeh, M. Zarinejad, T. a. Dean, Consolidation of Al particles through forward extrusion-equal channel angular pressing (FE-ECAP), Mater. Lett. 62 (2008) 3266–3268. doi:10.1016/j.matlet.2008.02.038.

[22] L. Kunčická, R. Kocich, J. Drápala, V.A. Andreyachshenko, FEM simulations and comparison of the ecap and ECAP-PBP influence on Ti6Al4V alloy's deformation behaviour, Metal 2013 22nd Int. Met. Mater. Conf. (2013) 391–396.

[23] F. Fereshteh-Saniee, M. Asgari, N. Fakhar, Specialized mechanical properties of pure aluminum by using non-equal channel angular pressing for developing its electrical applications, Appl. Phys. A. 122 (2016) 779. doi:10.1007/s00339-016-0305-3.

[24] R. Kocich, L. Kunčická, P. Král, A. Macháčková, Sub-structure and mechanical properties of twist channel angular pressed aluminium, Mater. Charact. 119 (2016) 75–83. doi:10.1016/j.matchar.2016.07.020.

[25] R. Kocich, L. Kunčická, M. Mihola, K. Skotnicová, Numerical and experimental analysis of twist channel angular pressing (TCAP) as a SPD process, Mater. Sci. Eng. A. 563 (2013) 86–94. doi:10.1016/j.msea.2012.11.047.

[26] L. Kunčická, R. Kocich, P. Král, M. Pohludka, M. Marek, Effect of strain path on severely deformed aluminium, Mater. Lett. 180 (2016) 280–283. doi:10.1016/j.matlet.2016.05.163.

[27] L.M. Hlaváč, R. Kocich, L. Gembalová, P. Jonšta, I.M. Hlaváčová, AWJ cutting of copper processed by ECAP, Int. J. Adv. Manuf. Technol. 86 (2016) 885–894. doi:10.1007/s00170-015-8236-2.

[28] B. Beausir, J.-J. Fundenberger, ATOM - Analysis Tools for Orientation Maps, Univ. Lorraine - Metz. (2015). http://atom-software.eu/.

[29] L.S. Tóth, Y. Estrin, R. Lapovok, C. Gu, A model of grain fragmentation based on lattice curvature, Acta Mater. 58 (2010) 1782–1794. doi:10.1016/j.actamat.2009.11.020.

[30] D.B. Williams, C.B. Carter, Diffraction from Crystals, in: Transm. Electron Microsc., Springer US, Boston, MA, 1996: pp. 237–249. doi:10.1007/978-1-4757-2519-3_16.

[31] O. Engler, V. Randle, Introduction to Texture Analysis, Macrotexture, Microtexture, and Orientation Mapping, 2nd ed., Taylor and Francis Group, 2010.

[32] R. Kocich, L. Kunčická, D. Dohnalík, A. Macháčková, M. Šofer, Cold rotary swaging of a tungsten heavy alloy: Numerical and experimental investigations, Int. J. Refract. Met. Hard Mater. 61 (2016) 264–272. doi:10.1016/j.ijrmhm.2016.10.005.

[33] M. Strobl, R.P. Harti, C. Grünzweig, R. Woracek, J. Plomp, Small Angle Scattering in Neutron Imaging — A Review, J. Imaging. 64 (2017) 2–15. doi:10.3390/jimaging3040064.

[34] L. Kunčická, R. Kocich, Structure Development after Twist Channel Angular Pressing, Acta Phys. Pol. A. 134 (2017) 681–685.

[35] L. Kunčická, R. Kocich, Natural ageing of aluminium processed by twist channel angular pressing, in: Proc. Fifth Intl. Conf. Adv. Civil, Struct. Mech. Eng. - CSM 2017, Institute of Research Engineers and Doctors, Zürich, 2017: pp. 7–11.

[36] R. Kocich, M. Greger, M. Kursa, I. Szurman, A. Macháčková, Twist channel angular pressing (TCAP) as a method for increasing the efficiency of SPD, Mater. Sci. Eng. A. 527 (2010) 6386–6392. doi:10.1016/j.msea.2010.06.057.

Figure captions

Fig. 1: Schematics of TCAP billet with locations for neutron diffraction analyses, individual scanning planes were perpendicular to extrusion axis in each individual point, for points 2 and 3 scanned plane crossed both points (a); photo of TCAP billet with microhardness indents (b).

Fig. 2: EBSD scan of unprocessed material, HAGBs highlighted in green (a); grain size distribution for unprocessed state (b); grain size distribution after single pass ECAP (c); grain

size distribution after single pass TCAP (d); grain size distribution after TCAP, two-years-aged (e), recrystallized fraction for two-years-aged TCAP sample (f).

Fig. 3: TEM images taken from samples: TCAP after processing (a); one-year-aged ECAP (b); one-year-aged TCAP (c); two-years-aged TCAP (d).

Fig. 4: Development of precipitates within two-years-aged TCAP, SEM image (a); TEM image (b).

Fig. 5: Residual stress within TCAP sample; after processing (a); after two years of natural ageing (b).

Fig. 6: Azimuthally averaged scattered data (a); SANS pattern from twist region (plane superimposed through point 1) (b); SANS pattern from plane superimposed through point 4 in outlet channel (c).

Fig. 7: Microhardness values across the two-years-aged sample.

Table captions

Table 1: Chemical compositions of precipitates depicted in Fig. 4b.

Table 2: Electric resistivity of TCAP samples in various conditions

HIGHLIGHTS

- Investigation of sub-structure development after twist channel angular pressing and ageing
- Natural ageing increased electric conductivity and mechanical properties
- Ultra-fine grains with high angle boundaries were formed
- Natural ageing led to reduction of residual stress